*Article*

# Ergodic Rate Analysis for Full-Duplex and Half-Duplex Networks with Energy Harvesting

**Bin Zhong** [1,†] **, Liang Chen** [1,†] **and Zhongshan Zhang** [2,*]

1 School of Information and Electrical Engineering, Hunan University of Science and Technology, Xiangtan 411201, China; zhongbin@hnust.edu.cn (B.Z.); kentchen@hnust.edu.cn (L.C.)
2 School of Cyberspace Science and Technology, Beijing Institute of Technology, Beijing 100081, China
* Correspondence: zhangzs@bit.edu.cn
† These authors contributed equally to this work and should be considered co-first authors.

**Abstract:** Considering energy harvesting, the ergodic data rates for both in band full-duplex (FD) and half-duplex (HD) wireless communications were studied. The analytic expressions of downlink and uplink ergodic rates for the proposed system were first derived with independent and identically distributed (i.i.d.) Rayleigh fading link. It was revealed that the uplink data rate can be improved by decreasing the downlink data rate. Furthermore, the uplink/downlink data rates are also shown to be influenced by some significance parameters, for example, the power split parameter and signal-to-noise ratio (SNR) (i.e., $P_S/\sigma^2$) of each link. Additionally, unlike the HD, the proposed FD node is capable of harvesting energy during the communication process; however, this is at the cost of performance loss induced by the residual self-interference (RSI), which is caused by the essence of simultaneous uplink and downlink transmissions in a single frequency band.

## 1. Introduction

With the increasing popularity of smart terminals, the shortage of wireless spectrum resources is becoming more and more prominent. Meanwhile, extending the lifetime of network devices has also become an important issue in this field.

Recently, in view of the limited spectral efficiency of the half-duplex (HD) node obtained by exchanging the signal for two-way communications with difference time slots, full-duplex (FD) technology has been widely regarded as an efficient way to improve spectral efficiency [1], although the performance of the latter is limited by the strength of the self-interference (SI) [2]. Furthermore, energy harvesting with simultaneous wireless information and power transfer (SWIPT) has been known as a promising technique for substantially increasing the lifetime of devices, which can be partially charged by the serving base station (BS) during its downlink data transmission phase [3,4]. In this paper, we assume that mobile devices can charge their power by exploiting the dissipated power of the BS, and the FD technique with energy harvesting capability is investigated. The ergodic data rate is shown to be substantially improved by employing in band FD mode due to its inherent bidirectional communication by using only one frequency band. It is shown that in the signal-to-noise ratio (SNR) range of [0, 24] dB, the FD mode always outperforms the HD mode in terms of ergodic data rate.

The main contributions of this paper include:

(1) The analytic expressions of downlink/uplink ergodic data rates for the FD/HD nodes with SWIPT are derived;
(2) The impact of power split parameter on energy harvesting is analyzed;
(3) The impact of self-interference cancellation capability with residual self-interference (RSI) coefficient λ on the FD node is studied.

The main paper is organized as follows: Section 2 provides related research. The system model of energy harvesting is proposed in Section 3. The analytic expressions of downlink and uplink ergodic data rates for both FD and HD modes in the SWIPT network are derived in Sections 4 and 5, respectively. Furthermore, the simulation results are shown in Section 6. Finally, Section 7 gives out the conclusions of this paper.

## 2. Related Work

Until now, SWIPT technology in HD networks has received extensive attention in the industry [5–14]. For instance, the cooperative SWIPT was proposed in [5], in which the near non-orthogonal multiple access (NOMA) users close to the source node are assumed to act as the energy harvesting HD relays for assisting remote users' data transmissions. In [6], Yuan Y. et al. study a novel cooperative NOMA access strategy, where central users act as relay cooperative edge users for data transmission, with central users gathering energy during the cooperative phase to optimize energy efficiency. In [7], Li G. et al. introduce optimal designs for HD relay-assisted NOMA networks. In [8], Zaidi S. K. et al. delve into SWIPT for single-user NOMA, deriving closed-form expressions for uplink and downlink ergodic data rates. In [9], Ding Z. et al. propose power allocation strategies in SWIPT networks to improve capacity by adjusting the power splitting factor. In [10], Hakimi A. et al. introduce a nonlinear energy harvesting model for NOMA cognitive relay network systems to rectify discrepancies between traditional linear models and real circuits in low-power and high-power regions. In [11], Liu C. P. et al. devise a nonlinear energy harvesting model for downlink transmission in cooperative NOMA systems with SWIPT, alongside an optimal power time allocation algorithm. In [12], Wang W. et al. exploit a nonlinear energy harvesting model to furnish SWIPT for NOMA users using unmanned aerial vehicles and ensure secure transmission for received users through controlled artificial interference. Moreover, the methods in [13,14] both make energy harvesting achievable. However, to the best of the authors' knowledge, SWIPT in FD networks has not been substantially studied in prior research.

## 3. System Model of Energy Harvesting
### 3.1. Channel Model

In this section, the investigation of a wireless communication network with SWIPT is described, where we assume that a user $U$ keeping a fixed distance $d$ to a source node $S$ is capable of communicating bi-directionally/directionally, as shown in Figure 1. In this system, the nodes are assumed to be equipped with no more than two antennas, enabling them to work in either HD or FD modes. In particular, all FD nodes are affected by RSI. Furthermore, we assume that the reciprocal Rayleigh fading channels between $S$ and $U$ (i.e., $h_{S,U}$) are independent and identically distributed (i.i.d.), i.e., $h_{S,U} \sim \mathrm{CN}(0, 1)$, where $\mathrm{CN}(0, 1)$ denotes a circularly symmetric complex Gaussian distribution with zero mean and unit variance. Hence, the power gain of channel between $S$ and $U$, as denoted by $|h_{S,U}|^2$, experiences exponential distribution with unit mean (i.e., $|h_{S,U}|^2 \sim \exp(1)$). Moreover, the additive white Gaussian noise (AWGN) found in all communication network nodes. In addition, the transmit power of $S$ (i.e., $P_S$) is assumed to be split by a power split coefficient $\alpha$ ($0 < \alpha < 1$). Therefore, a portion of split power $\alpha P_S$ can be employed for energy harvesting. Meanwhile, the remainder power, i.e., $P_{\mathrm{DL}} = (1-\alpha)P_S$, can be used for performing downlink communication.

Hence, the power of each user for uplink transmission is thus given by

$$P_U^{\mathrm{T}} = \frac{P_S \alpha \eta ||h_{S,U}||^2}{\varepsilon + d^\delta},$$

(1)

where $\varepsilon$ denotes a fixed parameter for ensuring a finite harvested energy and path loss, and $\delta$ stands for the path loss exponent, $\eta$ represents the energy harvesting efficiency (when $\eta = 1$, all the received power from the downlink is used for uplink transmission).
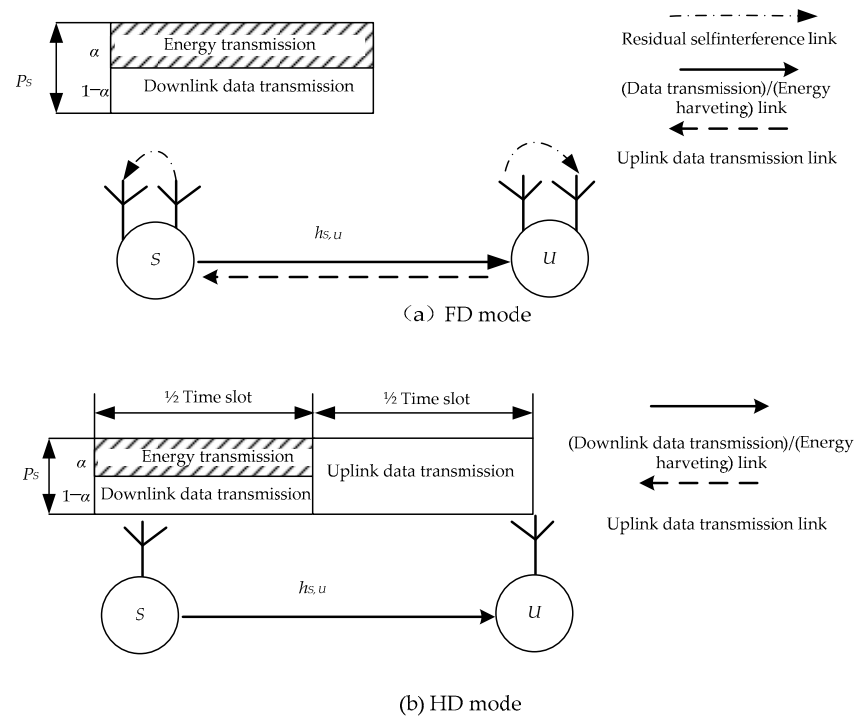
**Figure 1.** The proposed FD/HD networks with energy harvesting.

### 3.2. FD Transmission

(1) Downlink Signal Receiver for FD Transmission: When the nodes are working as FD mode, the downlink signal received at the $U$ can be given by

$$Y_{\text{FD}}^{\text{DL}} \to U = \frac{\sqrt{P_{\text{DL}}}h_{S,U}}{\sqrt{\varepsilon + d^{\delta}}}x + \sqrt{P_U^T \lambda_U}x' + n_U, \tag{2}$$

where $x$ ($/x'$) denotes the downlink (/uplink) signal transmitted by $S$ ($/U$), $\lambda_U$ represents the RSI power coefficient for full-duplex node $U$, and $n_U$ denotes the AWGN at $U$ with $n_U \sim \text{CN}(0, \sigma_U^2)$.

The downlink signal-to-interference-plus-noise ratio (SINR) at $U$ can thus be expressed as

$$\gamma_{\text{FD}}^{\text{DL}} = \frac{b_{1,1}|h_{S,U}|^2}{c_1 \lambda_U |h_{S,U}|2 + 1}, \tag{3}$$

where $b_{1,1} = \frac{P_{\text{DL}}}{\sigma_U^2(\varepsilon + d^{\delta})}$, and $c_1 = \frac{P_S \alpha}{\sigma_U^2(\varepsilon + d^{\delta})}$ denote the power-to-noise ratio (PNR) for downlink data transmission and energy transmission at the user of interest, respectively.

(2) Uplink Signal Receiver for FD Transmission: The uplink signal received by $S$ is given by

$$Y_{\text{FD}}^{\text{UP}} \to S = \frac{\sqrt{P_U^{\text{T}}}x'h_{S,U}}{\sqrt{\varepsilon + d^{\delta}}} + \sqrt{P_{\text{DL}}\lambda_0}x + n_S, \tag{4}$$

where $\lambda_0$ denotes the RSI power coefficient for FD node $S$, and $n_S$ denotes the AWGN at $S$ with $n_S \sim \text{CN}(0, \sigma_S^2)$.

The received SINR of $x'$ at $S$ is thus given by

$$\gamma_{FD}^{UP} = a_1 \left| h_{S,U} \right| 4, \tag{5}$$

where $a_1 = \frac{\alpha P_S}{(\varepsilon + d^{\delta})^2 (\lambda_0 P_{DL} + \sigma_S^2)}$.

*3.3. HD Transmission*

(1) Downlink Signal Receiver for HD Transmission: When the nodes are working at the HD mode, the downlink signal received by the $U$ can be given by

$$Y_{HD}^{DL} \to U = \frac{\sqrt{P_{DL}}h_{S,U}}{\sqrt{\varepsilon + d^\delta}}x + n_U. \tag{6}$$

Furthermore, the SINR at $U$ for downlink transmission is

$$\gamma_{HD}^{DL} = b_{1,1}\Big|h_{S,U}\Big|2. \tag{7}$$

(2) Uplink Signal Receiver for HD Transmission: The uplink signal received by $S$ is

$$Y_{HD}^{UP} \to S = \frac{\sqrt{P_U^T}x'h_{S,U}}{\sqrt{\varepsilon + d^\delta}} + n_S. \tag{8}$$

Thus, the received uplink SINR at $S$ can be expressed as

$$\gamma_{HD}^{UP} = a_2\Big|h_{S,U}\Big|4, \tag{9}$$

where $a_2 = \frac{\alpha P_S}{(\varepsilon + d^\delta)^2 \sigma_S^2}$.

## 4. Downlink Ergodic Rate

*4.1. Downlink Ergodic Rate for FD Transmission*

By applying Equation (4.337.2) [15], the downlink ergodic data rate for FD-SWIPT based transmission can be derived as

$$
\begin{aligned}
R_{FD}^{DL} &= \mathbb{E}\left[\log_2\left(1 + \frac{b_{1,1}|h_{S,U}|^2}{c_1\lambda_U|h_{S,U}|2+1}\right)\right] \\
&= \frac{1}{\ln 2}\int_0^{+\infty}[\ln(1 + (c_1\lambda_U + b_{1,1})x) - \ln(1 + c_1\lambda_U x)]e^{-x}dx \\
&= [\exp(\xi)E_1(\xi) - \exp(\zeta)E_1(\zeta)]/\ln 2,
\end{aligned}
\tag{10}
$$

where $\mathbb{E}[\cdot]$ stands for the statistical expectation operation, $\xi = \frac{1}{c_1\lambda_U + b_{1,1}}$, $\zeta = \frac{1}{c_1\lambda_U}$, and $E_1(x) = \int_x^{+\infty} e^{-t}/t\, dt = -\text{Ei}(-x)$ in which $\text{Ei}(\cdot)$ denotes the exponential integral function: Equation (8.211.1) [15].

*4.2. Downlink Ergodic Rate for HD Transmission*

Similarly, the downlink average ergodic rate for the HD-SWIPT-based transmission can be given by

$$
\begin{aligned}
R_{HD}^{DL} &= \frac{1}{2\ln 2}\int_0^{+\infty}\ln(1 + b_{1,1}x)e^{-x}dx \\
&= \frac{1}{2\ln 2}\exp\left(\frac{1}{b_{1,1}}\right)E_1\left(\frac{1}{b_{1,1}}\right).
\end{aligned}
\tag{11}
$$

## 5. Uplink Ergodic Rate

*5.1. Uplink Ergodic Rate for FD Transmission*

By utilizing Equation (4.338.1) [15], the uplink ergodic data rate for FD-SWIPT based transmission can be given by

$$
\begin{aligned}
R_{FD}^{UP} &= \frac{1}{\ln 2}\int_0^{+\infty}\ln(1 + a_1 x^2)e^{-x}dx \\
&= \frac{2}{\ln 2}\left[-\sin\left(\frac{1}{\sqrt{a_1}}\right)\text{si}\left(\frac{1}{\sqrt{a_1}}\right) - \cos\left(\frac{1}{\sqrt{a_1}}\right)\text{ci}\left(\frac{1}{\sqrt{a_1}}\right)\right],
\end{aligned}
\tag{12}
$$

where $\mathrm{si}(x) = -\int\limits_x^{+\infty} \dfrac{\sin(t)}{t} dt$; Equation (8.230.1) [15], and $\mathrm{ci}(x) = -\int\limits_x^{+\infty} \dfrac{\cos(t)}{t} dt$; Equation (8.230.2) [15].

*5.2. Uplink Ergodic Rate for HD Transmission*

Likewise, the uplink ergodic data rate for HD-SWIPT-based transmission can be given by

$$R_{\mathrm{HD}}^{\mathrm{UP}} = \left[ -\sin\left(\frac{1}{\sqrt{a_2}}\right) \mathrm{si}\left(\frac{1}{\sqrt{a_2}}\right) - \cos\left(\frac{1}{\sqrt{a_2}}\right) \mathrm{ci}\left(\frac{1}{\sqrt{a_2}}\right) \right] / \ln 2. \tag{13}$$

## 6. Simulation Results

Here, we study the uplink/downlink ergodic data rates for both FD and HD communication networks by considering energy harvesting. The derived exact analytic expressions are validated by using a numerical evaluation via a Monte Carlo simulation, as shown in Figures 2 and 3. Furthermore, the amount of SI is assumed to be suppressed in all terminals, i.e., $\lambda_0 = \lambda_U = \lambda$. In addition, the power of AWGN at both the user and $S$ is identical, i.e., $\sigma_S^2 = \sigma_U^2 = \sigma^2$.

In the following, in each figure, all curves are depicted as a function of SNR (i.e., $P_S/\sigma^2$). Furthermore, we also assumed that $\delta = 2.8$ and $\varepsilon = 1$. Note that the proposed analysis is also applicable for the other parameters. For variant $d$ values, the far distance implies larger path loss. Therefore, both the downlink rate and uplink rate are lower with far distance under the FD mode, as shown in Figures 4 and 5. Furthermore, the HD mode is similar. In the following simulation, we assumed a fixed path loss with $d = 1.5$.
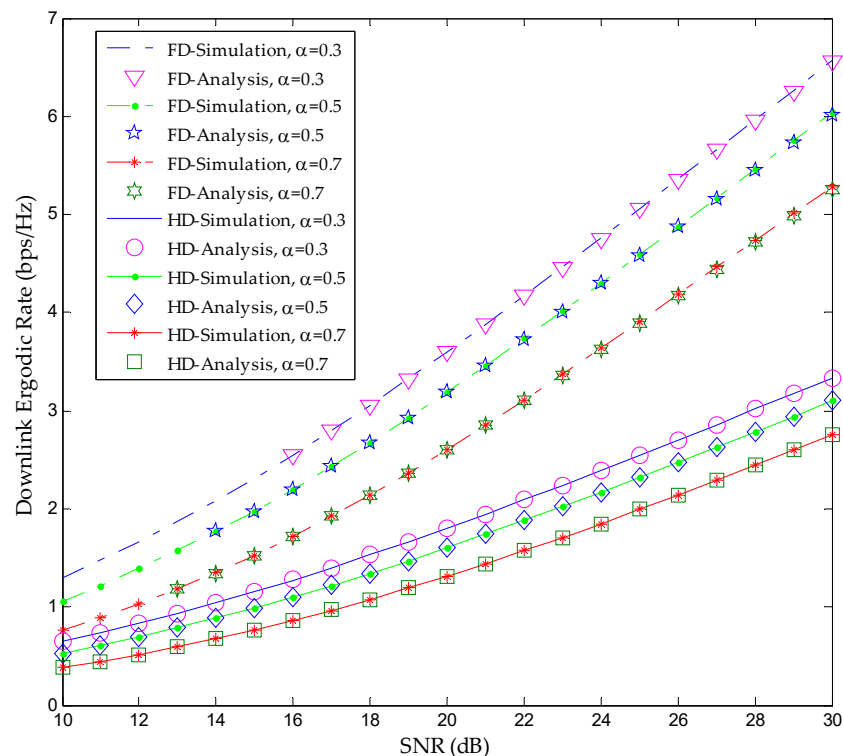


**Figure 2.** Downlink ergodic rate with different values of $\alpha$.

When keeping $\lambda = 0.001$ unchanged, for different $\alpha$, a smaller $\alpha$ implies a higher downlink transmission power, corresponding to a higher downlink data rate, as shown in Figure 2. Furthermore, increasing SNR implies that the quality of channel for users is improved, thus allowing users with higher SNR to obtain a higher data rate. In addition, in low SNR, the FD mode is superior to the HD mode.
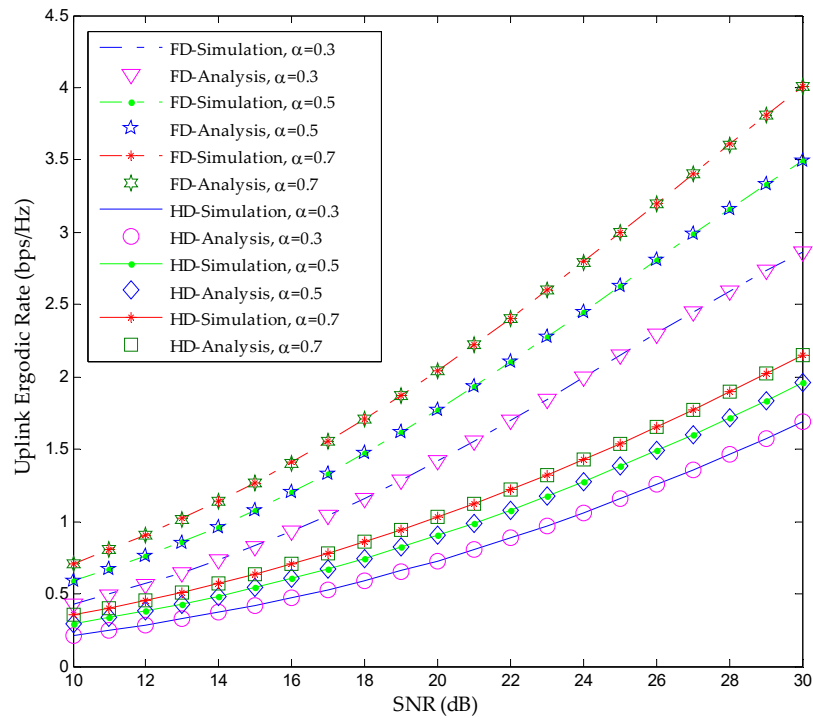
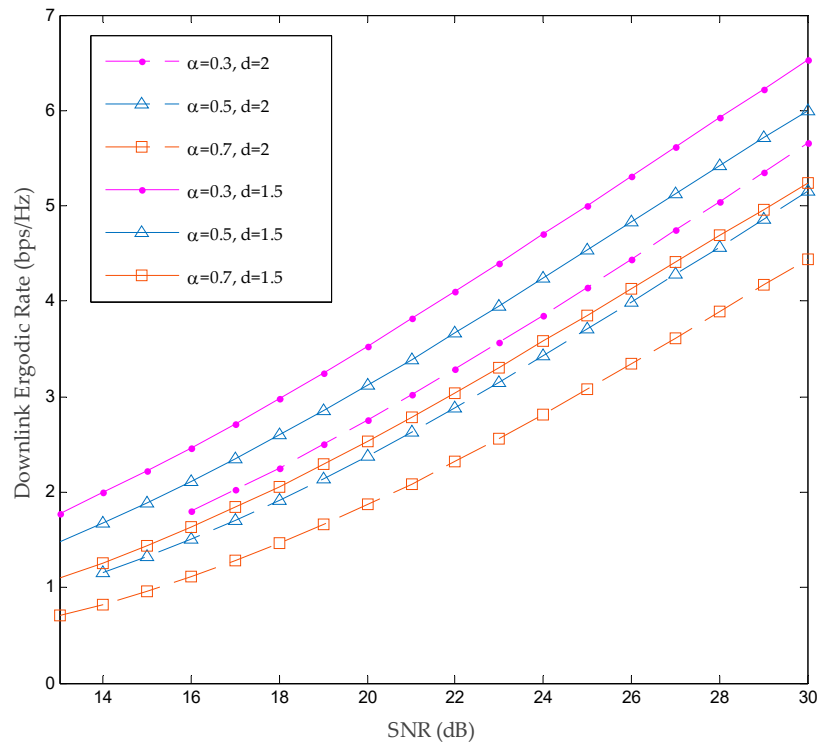**Figure 3.** Uplink ergodic rate with different values of $\alpha$.



**Figure 4.** Downlink ergodic rate with different values of $d$.

In Figure 6, it is shown that providing a higher power to the energy harvesting user will improve the uplink data rate. Furthermore, the uplink data rate can be improved by the cost of the decreasing downlink data rate. Thus, the data rates in both downlink and uplink transmissions can be adjusted by changing $\alpha$, demonstrating the benefits of employing SWIPT. In addition, by increasing $\alpha$ from 0 to 1, the uplink rate can be improved at the cost of eroding the downlink date rate.
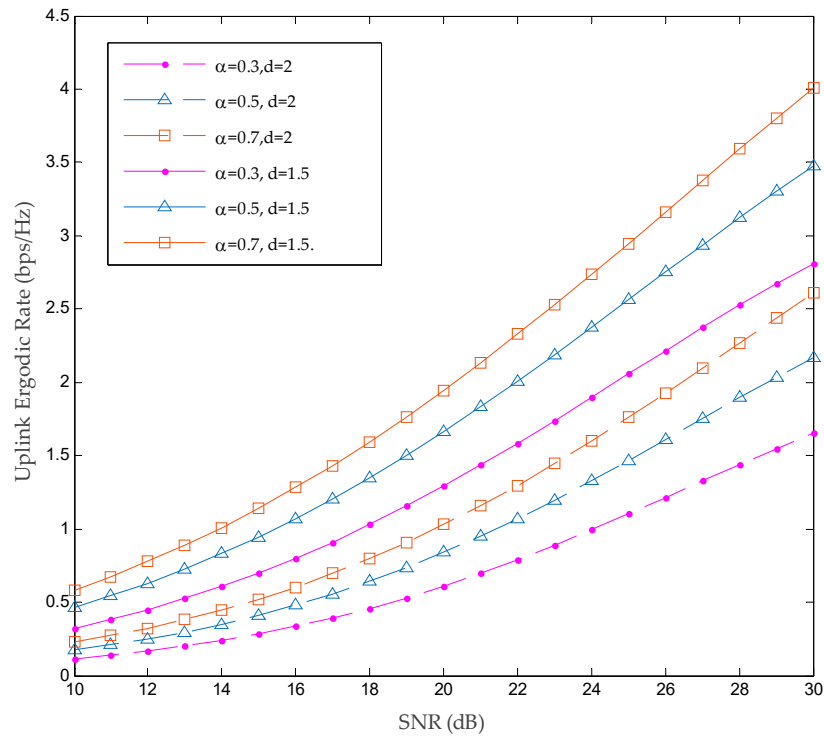
**Figure 5.** Uplink ergodic rate with different values of *d*.
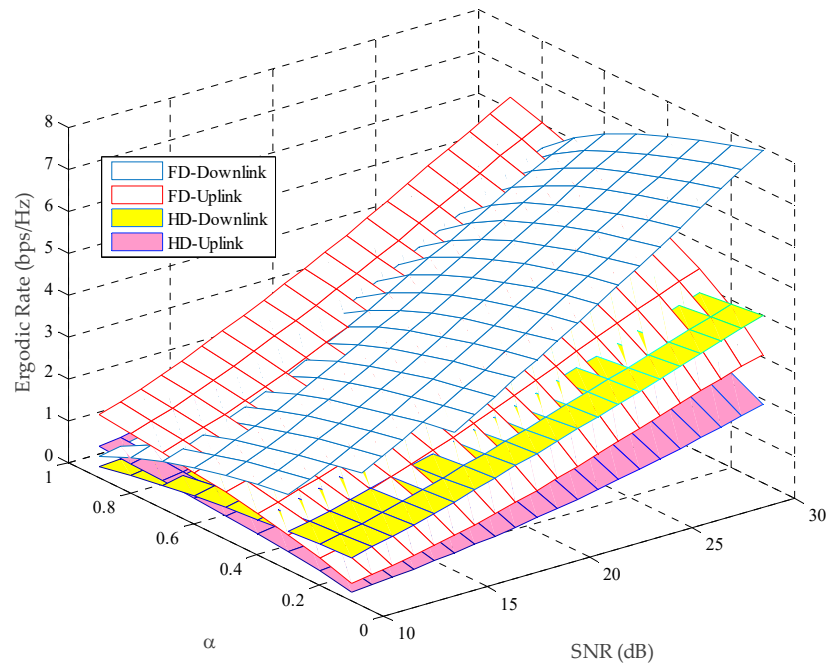


**Figure 6.** Ergodic rate with different values of α and SNR.

By keeping α = 0.5 unchanged, for variant λ values under the FD mode, a smaller λ implies a lower SI power, showing that the downlink date rate becomes higher, as shown in Figure 7. Generally speaking, the FD mode with a stronger SI suppressing ability is superior to the HD mode. Moreover, by increasing λ, the attainable performance gain being obtained by FD mode will be lost due to the strong RSI power.

By keeping λ = 0.001 unchanged, for variant α values, employing a high α value implies obtaining a higher energy harvesting transmission power, corresponding to a higher uplink date rate, as shown in Figure 3.
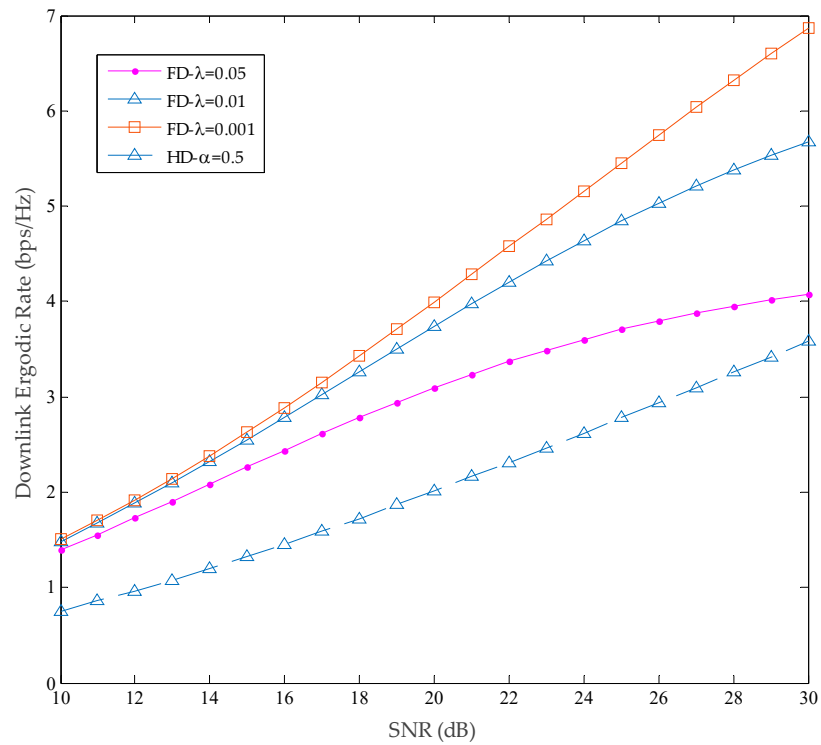
**Figure 7.** Downlink ergodic rate with different values of $\lambda$.

Similar to the downlink ergodic date rate, the uplink ergodic date rate for variant $\lambda$ values under the FD mode is shown in Figure 8. It shows that the SIC capability will always dominate the performance of the SWIPT networks, or in other words, the RSI power determines whether the FD is superior to HD or not in terms of the attainable data rate. Moreover, in the SNR range of [0, 24] dB, the FD mode always outperforms the HD mode in the proposed systems in terms of both downlink and uplink ergodic rates.
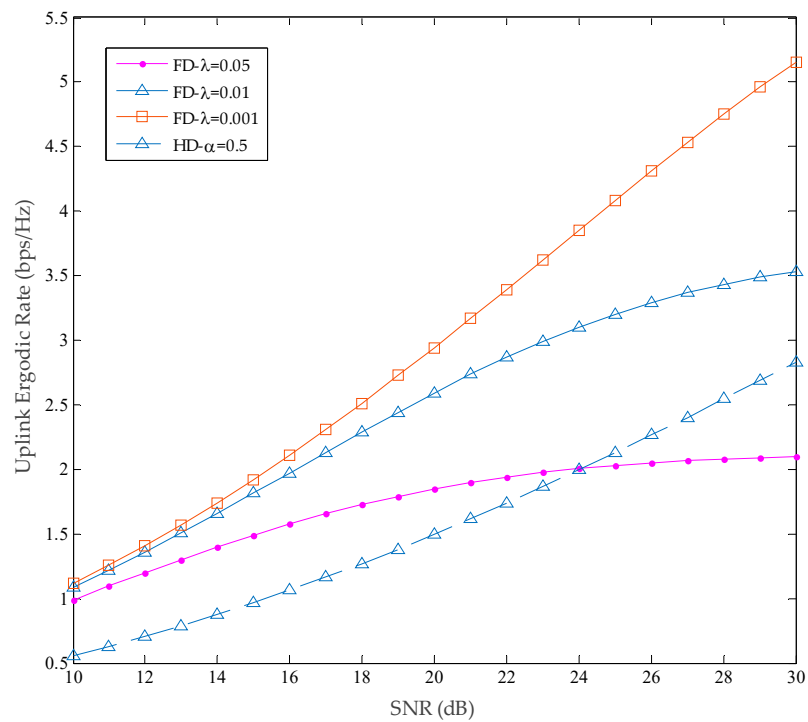


**Figure 8.** Uplink ergodic rate with different values of $\lambda$.

## 7. Conclusions

The ergodic data rates in the proposed SWIPT-aided wireless networks systems were studied by taking the FD (/HD) mode over Rayleigh fading links into account. The analytic expressions of downlink and uplink data rate were derived, followed by validating the proposed theoretical analytic expressions using simulations. Furthermore, it was also displayed that some critical parameters (such as the average SNR of the links, the power of residual self-interference $\lambda$, the power split parameter $\alpha$, etc.) may substantially impact both the uplink and downlink date rates of the proposed energy harvesting networks system.

## References

1. Hu, H.; Liu, C.; Chang, K. Full-Duplex Heterogeneous Networks: Ergodic Rate Analysis with Realistic Interference Modeling. In Proceedings of the 2017 IEEE Wireless Communications and Networking Conference (WCNC), San Francisco, CA, USA, 19–22 March 2017; pp. 1–6.
2. Zhang, Z.; Long, K.; Vasilakos, A.V.; Hanzo, L. Full-Duplex Wireless Communications: Challenges, Solutions and Future Research Directions. *Proc. IEEE* **2016**, *104*, 1369–1409. [CrossRef]
3. Wang, D.; Zhang, R.; Cheng, X.; Yang, L. Capacity-Enhancing Full Duplex Relay Networks Based on Power-Splitting (PS-)SWIPT. *IEEE Trans. Veh. Technol.* **2017**, *66*, 5445–5450. [CrossRef]
4. Zeng, Q.; Zheng, Y.; Zhong, B.; Zhang, Z. Minimum Transmission Protocol for Full-Duplex Systems with Energy Harvesting. *IEEE Commun. Lett.* **2019**, *23*, 382–385. [CrossRef]
5. Liu, Y.; Ding, Z.; Elkashlan, M.; Poor, H.V. Cooperative Non-Orthogonal Multiple Access with Simultaneous Wireless Information and Power Transfer. *IEEE J. Sel. Areas Commun.* **2016**, *34*, 938–953. [CrossRef]
6. Yuan, Y.; Xu, Y.; Yang, Z.; Xu, P.; Ding, Z. Energy Efficiency Optimization in Full-Duplex User-Aided Cooperative SWIPT NOMA Systems. *IEEE Trans. Commun.* **2019**, *67*, 5753–5767. [CrossRef]
7. Li, G.; Mishra, D.; Hu, Y.; Atapattu, S. Optimal Designs for Relay-Assisted NOMA Networks with Hybrid SWIPT Scheme. *IEEE Trans. Commun.* **2020**, *68*, 3588–3601. [CrossRef]
8. Zaidi, S.K.; Hasan, S.F.; Gui, X. Evaluating the Ergodic Rate in SWIPT-Aided Hybrid NOMA. *IEEE Commun. Lett.* **2018**, *22*, 1870–1873. [CrossRef]
9. Ding, Z.; Perlaza, S.M.; Esnaola, I.; Poor, H.V. Power Allocation Strategies in Energy Harvesting Wireless Cooperative Networks. *IEEE Trans. Wirel. Commun.* **2014**, *13*, 846–860. [CrossRef]
10. Hakimi, A.; Mohammadi, M.; Mobini, Z.; Ding, Z. Full-Duplex Non-Orthogonal Multiple Access Cooperative Spectrum-Sharing Networks with Non-Linear Energy Harvesting. *IEEE Trans. Veh. Technol.* **2020**, *69*, 10925–10936. [CrossRef]
11. Liu, C.P.; Zhang, L.; Chen, Z.; Li, S. Power-Time Resource Allocation for Downlink SWIPT-Assisted Cooperative NOMA Systems. *Sci. China Inf. Sci.* **2023**, *66*, 152303. [CrossRef]
12. Wang, W.; Tang, J.; Zhao, N.; Liu, X.; Zhang, X.Y.; Chen, Y.; Qian, Y. Joint Precoding Optimization for Secure SWIPT in UAV-Aided NOMA Networks. *IEEE Trans. Commun.* **2020**, *68*, 5028–5040. [CrossRef]
13. Bijak, J.; Sciuto, G.L.; Kowalik, Z.; Lasek, P.; Szczygieł, M.; Trawiński, T. Magnetic Flux Density Analysis of Magnetic Spring in Energy Harvester by Hall-Effect Sensors and 2D Magnetostatic FE Model. *J. Magn. Magn. Mater.* **2023**, *579*, 170796. [CrossRef]
14. Sciuto, G.L.; Bijak, J.; Kowalik, Z.; Szczygieł, M.; Trawiński, T. Displacement and Magnetic Induction Measurements of Energy Harvester System Based on Magnetic Spring Integrated in the Electromagnetic Vibration Generator. *J. Vib. Eng. Technol.* **2024**, *12*, 3305–3320. [CrossRef]
15. Gradshteyn, I.S.; Ryzhik, I.M. *Table of Integrals, Series, and Products*, 7th ed.; Academic Press: New York, NY, USA, 2007.